

7. J. O. Hinze, Turbulence, McGraw-Hill (1960).
8. M. A. Vorontsov and V. N. Shal'gauzen, Principles of Adaptive Optics [in Russian], Moscow (1985).

VISCOUS LIQUID FLOW IN THE INITIAL PORTION
OF A PERMEABLE CHANNEL WITH TRANSVERSE SLOT

A. S. Lebedev and F. F. Spiridonov

UDC 532.542:536.42

The problem of flow in the initial segment of a permeable channel with transverse impermeable slot is solved. Behavior of the solution with change in geometric parameters and characteristic injection Reynolds number is analyzed.

1. Flow in channels with permeable walls has recently attracted the ever greater attention of researchers. This is due to the importance of its practical applications. Flow of this type is found, for example, in gas motion in plasmotrons with porous electrodes, liquid motion in wells, in intense sublimation and condensation in a number of chemical technology processes, etc.

The majority of studies have considered developed flows in circular cylindrical [1-4] or annular [5, 6] channels. A number of investigators [7-9] have observed that distributed draft into the channel significantly increases the value of the critical Reynolds number for transition from a laminar to a turbulent flow regime, as compared to flow in a conventional tube. In addition it has been shown that conditions in the initial segment of the channel by its forward face affect the transition.

Significantly fewer studies [10-12] have considered flows in initial sections of permeable channels. In [10] a numerical modeling of flow in the initial segment of a planar channel was performed for initial injection Reynolds numbers in the range $10 \leq R_b \leq 300$. Flow in a planar channel with permeable transverse slot located near the forward face was considered for the same R_b range in [11]. Flow in the initial section of a planar channel with impermeable slot near its face was studied in [12] for the range $100 \leq R_b \leq 1000$. The present study will numerically model flow in the initial segment of a planar, circular, or annular channel (Fig. 1) with an impermeable transverse slot for change in slot geometric parameters and injection Reynolds numbers in the range $10 \leq R_b \leq 3000$.

The liquid is assumed incompressible with a constant dynamic viscosity coefficient.

2. The equations defining the flow in dimensionless form are

$$y^{2v} \left[\frac{\partial}{\partial z} \left(\frac{\omega}{y^v} \frac{\partial \Psi}{\partial y} \right) - \frac{\partial}{\partial y} \left(\frac{\omega}{y^v} \frac{\partial \Psi}{\partial z} \right) \right] - R_b^{-1} \left\{ \frac{\partial}{\partial z} \left[y^{3v} \frac{\partial}{\partial z} \left(\frac{\omega}{y^v} \right) \right] + \frac{\partial}{\partial y} \left[y^{3v} \frac{\partial}{\partial y} \left(\frac{\omega}{y^v} \right) \right] \right\} = 0, \quad (1)$$

$$\frac{\partial}{\partial z} \left(\frac{1}{y^v} \frac{\partial \Psi}{\partial z} \right) + \frac{\partial}{\partial y} \left(\frac{1}{y^v} \frac{\partial \Psi}{\partial y} \right) = -\omega; \quad R_b = \rho^{\circ} q_b^{\circ} \Delta^{\circ} / \mu^{\circ}.$$

On the impermeable boundaries $\Psi = 0$, while on the permeable boundary $\Psi = -R_2^v(z - b)$. The values of ω on the permeable ($y = R_2$) and impermeable boundaries are calculated during solution of the problem using the condition of absence of slippage, while on the right-hand boundary ($L \gg 1$) the values of Ψ and ω are calculated by extrapolation from the calculation region with the assumption of absence of longitudinal diffusion (for details, see [13, 14]). As length and velocity scales in Eq. (1) we use the channel width $\Delta^{\circ} = R_2^{\circ} - R_1^{\circ}$ and draft velocity q_b° .

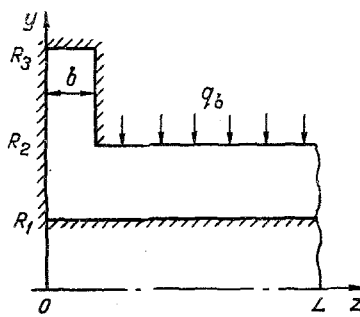


Fig. 1. Diagram of flow region.

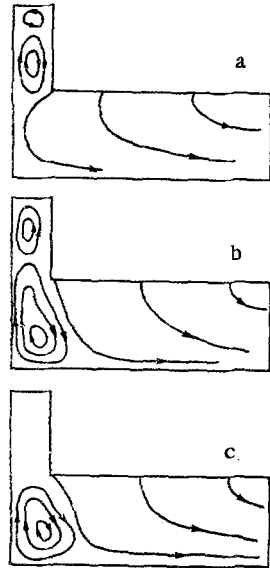


Fig. 2

Fig. 2. Change in flow structure with increase in R_1 : $R_1 = 0$ (a); $R_1 = 5$ (b); $R_1 > 7$ (c).

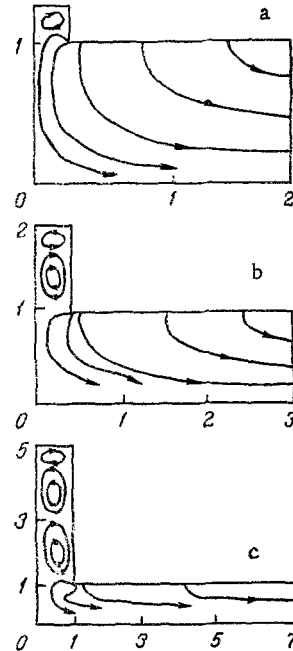


Fig. 3

Fig. 3. Change in flow structure with increase in h/b : $h/b = 1$ (a); 2 (b); 4 (c).

The problem thus formulated was solved numerically by a finite difference method [13] using nonuniform grids (compressed toward the boundaries of the region) for the range $10 \leq R_b \leq 3000$ and $0 \leq R_1 \leq 100$. Vorticity values in the flow field were calculated with a relaxation coefficient of 0.5, and on the boundaries with a coefficient of 0.1, which stabilized the calculation process. At the internal angular point the ω values were calculated with consideration of the recommendations of [14]. The rate of convergence was increased by almost an order of magnitude as compared to the method of [13] by organizing the relaxation cyclical process with Chebyshev parameters for Ψ . Stable, grid-size independent solutions were obtained on grids for 40×50 to 30×150 . The criterion for convergence was maximum relative discrepancy of the vorticity in two successive iterations $|\delta\omega| \leq 1 \cdot 10^{-4}$. Additionally, on the boundary $z = L$ the solution obtained was monitored for correspondence to the known analytical solutions [1, 5].

3. In performing the calculations the dependence of flow structure on the quantities R_1 , $h = R_3 - R_2$, b , and R_b was studied. The channel width was maintained constant ($\Delta = 1$). Figure 2 shows the character of the change in flow structure with change in R_1 for $R_b = 2000$. Slot height and width values for this case are $h = 1$, $b = 0.5$. The calculations showed that the flow structure was practically independent of the value of the characteristic injection Reynolds number for change in the latter over the range $100 \leq R_b \leq 3000$. Decrease in b for fixed h (like increase in h for fixed b) for $b \leq 1$ and $h \geq 1$ lead to practically identical results: the quantity of vortices near the forward face of the channel increases (for

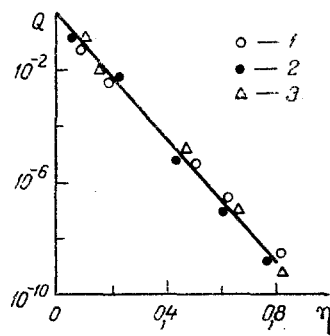


Fig. 4. Recirculation zone intensity vs slot height ($R_b \geq 100$):
1) $R_b = 100$; 2) 1000; 3) 3000.

$R_1 \leq 7$). For $R_1 > 7$ (flow approaching planar) the vortex structures are located in the channel, with slot width and height apparently playing an insignificant role. On the whole these results agree fairly well with the experimental and calculated data presented in [12]. It is interesting that in the axisymmetric case ($R_1 = 0$) independent of whether OZ is the axis of symmetry or the impermeable boundary, for the indicated R_b range recirculation flow in the vicinity of the point 0 is not observed. In the planar case ($v = 0$ or $R_1 \gg 1$) in the vicinity of the point 0 there is a recirculation flow, the dimensions of which at $h = 0$ and $b = 0$ are defined by a dependence on R_b close to that presented in [10].

Development of the flow structure in the range $100 \leq R_b \leq 3000$ for $R_1 = 0$ with increase in the ratio h/b is shown in Fig. 3. The data presented indicate that the quantity of recirculating zones in the slot increases with increase in the ratio h/b . The dependence of the number of such zones on h/b is close to linear.

It is of interest to find the dependence of the intensity Q of the circulation zones on the coordinate $\eta = (y - R_2)/(R_3 - R_2)$, measured along the slot. By the intensity Q we understand the mean integral over the volume of an individual vortex of its rotation velocity. This dependence, obtained by processing the calculated data and valid for $R_b > 100$, is shown in Fig. 4, whence it is evident that circulation zone intensity falls off very rapidly with slot height. With accuracy sufficient for practical use this dependence can be approximated by the expression $\eta = -0.1 \ln Q$.

NOTATION

z, y , rectangular (cylindrical) coordinates; R_1, R_2, R_3 , characteristic radii of channel and slot; Δ , channel width; b, h , slot width and height; L , channel length; R_b , characteristic injection Reynolds number; q_b^0 , draft velocity into channel; ρ^0, μ^0 , liquid density and viscosity; $^\circ$, degree (denotes dimensional quantity); ω, Ψ , vorticity, flow function; v , subscript ($v = 0, 1$ is planar or axisymmetric flows); $\delta\omega$, maximum relative discrepancy of vorticity for two subsequent iterations; $\eta = (y - R_2)/(R_3 - R_2)$ coordinate measured along slot; Q , recirculation zone intensity.

LITERATURE CITED

1. A. S. Berman, J. Appl. Phys., 24, No. 9, 1232-1235 (1953).
2. G. Taylor, Proc. R. Soc., London, A234, No. 1199, 456-475 (1956).
3. S. W. Yuan, J. Math. Phys., 38, No. 3, 166-171 (1959).
4. R. M. Olson and E. R. Eckert, Proc. Am. Soc. Mech. Eng., Ser. E, Appl. Mech., 38, No. 1, 7-20 (1966).
5. R. M. Terrill, Appl. Sci. Res., 17, No. 3, 204-222 (1967).
6. V. I. Zinchenko and I. P. Fedorova, Izv. Akad. Nauk SSSR, Mekh. Zhidk. Gaza, No. 3, 135-139 (1976).
7. V. N. Varapaev and V. I. Yagodkin, Izv. Akad. Nauk SSSR, Mekh. Zhidk. Gaza, No. 5, 91-95 (1969).
8. V. N. Varapaev and V. I. Yagodkin, Izv. Akad. Nauk SSSR, Mekh. Zhidk. Gaza, No. 4, 125-129 (1970).
9. V. M. Eroshenko, L. I. Zaichik, and V. B. Rabovsikii, Zh. Prikl. Mekh. Tekh. Fiz., No. 3, 82-86 (1984).
10. V. N. Varapaev, Izv. Akad. Nauk SSSR, Mekh. Zhidk. Gaza, No. 4, 178-181 (1969).
11. S. V. Kalinina and F. F. Spiridonov, Boundary Layers Under Complex Conditions [in Russian], Novosibirsk (1984), pp. 28-33.

12. V. I. Alimpiev, A. L. Sorokin, and V. G. Safonov, Boundary Layers under Complex Conditions [in Russian], Novosibirsk (1984), pp. 5-15.
13. A. D. Gosmen, V. M. Pan, A. K. Ranchel, et al., Numerical Methods for Study of Viscous Liquid Flows [in Russian], Moscow (1972).
14. P. J. Roache, Computational Fluid Dynamics, Hermosa (1976).

CALCULATION OF NOZZLE FLOW WITH MIXING IN THE PRESENCE
OF A STRONG VORTICITY EFFECT

V. I. Vasil'ev

UDC 532.522.2:519.633

A method of calculating the essentially three-dimensional turbulent flow in a mixing channel is proposed. The results of calculating the nozzle flow behind a mixer is presented.

1. In mixing nozzles, mixers generally of the tab type, are used to intensify the mixing process. The distribution of the parameters behind a mixer at the nozzle inlet is circumferentially nonuniform, and the flow is essentially three-dimensional. Experiments [1] have also shown that the flow over a curved mixer surface may create intense longitudinal vortices, under whose influence one of the streams separates into a number of jets.

The calculation of nozzle flows behind mixers was the subject of studies [2, 3]. In [2] the Patankar-Spalding method [4], intended for the numerical integration of the parabolized Navier-Stokes equations, was employed. The calculations were compared with the experimental data, but the lack of information on the cross flow fields at the mixer exit face made it impossible to obtain good agreement. In [3] the experimental data of [1] were used as the conditions at the mixer exit and the results of the calculations were found to be in satisfactory qualitative and quantitative agreement with experiment. These calculations made use of a method [5] originally developed for investigating flows in curved channels. The parameter distributions were found by numerical integration of the equations written in a coordinate system moving with the inviscid gas streamlines in a nozzle of the same geometry but without mixing. The pressure distribution was represented as the sum of the pressure fields in the inviscid gas flow and a correction for mixing. In this case the calculations are more complicated than when the method adopted in [2] is employed.

Our aim was to show that when the true nature of the cross flows at the mixer exit is taken into account, the parabolized Navier-Stokes equations make it possible to describe the mixing process in the nozzle. The cross flows are calculated using the approach proposed in [6], extended to the case of compressible gas flows. For describing the cross flows due to vorticity it is also proposed to employ simplified relations that are exact in the limiting case - the mixing of flows with only slightly different parameters.

2. The parabolized Navier-Stokes equations describe weakly expanding flows, i.e., flows in which the parameters in a preferred direction vary much more weakly than in the transverse section. For subsonic perfect gas flows with constant specific heats in the cylindrical coordinate system in which x is the axial coordinate in the preferred direction these equations take the form:

$$\frac{\partial \rho u^2}{\partial x} + \operatorname{div}(\rho \mathbf{V}u) = -\frac{dP}{dx} + \operatorname{div}(\rho \nu_t \nabla u), \quad (1)$$

$$\frac{\partial \rho uv}{\partial x} + \operatorname{div}(\rho \mathbf{V}v) = -\frac{\partial p}{\partial y} + \frac{1}{y} \frac{\partial}{\partial y} (y \tau_{yy}) + \frac{1}{y} \frac{\partial \tau_{y\theta}}{\partial \theta} - \frac{\tau_{\theta\theta}}{y}, \quad (2)$$